

UCSF

UC San Francisco Previously Published Works

Title

A Preliminary Study of Left Ventricular Rotational Mechanics in Children with Noncompaction Cardiomyopathy: Do They Influence Ventricular Function?

Permalink

<https://escholarship.org/uc/item/0xf2s1ws>

Journal

Journal of the American Society of Echocardiography : official publication of the American Society of Echocardiography, 31(8)

ISSN

0894-7317

Authors

Nawaytou, Hythem M
Montero, Andrea E
Yubbu, Putri
et al.

Publication Date

2018-08-01

DOI

10.1016/j.echo.2018.02.015

Peer reviewed

A Preliminary Study of Left Ventricular Rotational Mechanics in Children with Noncompaction Cardiomyopathy: Do They Influence Ventricular Function?

Hythem M. Nawaytou, MBBCH, Andrea E. Montero, MD, Putri Yubbu, MD, Renzo J. C. Calderón-Anyosa, MD, Tomoyuki Sato, MD, Matthew J. O'Connor, MD, Kelley D. Miller, CRNP, Philip C. Ursell, MD, Julien I. E. Hoffman, MD, and Anirban Banerjee, MD, FACC, Philadelphia, Pennsylvania; and San Francisco, California

Background: Current diagnostic criteria for noncompaction cardiomyopathy (NCC) lack specificity, and the disease lacks prognostic indicators. Reverse apical rotation (RAR) with abnormal rotation of the cardiac apex in the same clockwise direction as the base has been described in adults with NCC. The aim of this study was to test the hypothesis that RAR might differentiate between symptomatic NCC and benign hypertrabeculations and might be associated with ventricular dysfunction.

Methods: Echocardiograms from 28 children with NCC without cardiac malformations were prospectively compared with those from 29 age-matched normal control subjects. A chart review was performed to identify the patients' histories and clinical characteristics. Speckle-tracking was used to measure longitudinal strain, circumferential strain, and rotation.

Results: RAR occurred in 39% of patients with NCC. History of left ventricular (LV) dysfunction or arrhythmia was universal in, but not exclusive to, patients with RAR. Patients with RAR had lower LV longitudinal strain but similar ejection fractions compared with patients without RAR (median, -15.6% [interquartile range, -12.9% to -19.3%] vs -19% [interquartile range, -14.5% to -21.9%], $P < .01$; 53% [interquartile range, 43% to 68%] vs 61% [interquartile range, 58% to 67%], $P = .08$). Only a pattern of contraction with RAR, early arrest of twisting by mid-systole, and premature untwisting was associated with lower ejection fraction (46%; interquartile range, 43% to 52%; $P = .006$).

Conclusions: RAR is not a sensitive but is a specific indicator of complications in children with NCC. Therefore, RAR may have prognostic rather than diagnostic value. Premature untwisting of the left ventricle during ejection may be an even more worrisome indicator of LV dysfunction. (J Am Soc Echocardiogr 2018; ■: ■-■.)

Keywords: Cardiomyopathy, Mechanics, Noncompaction, Pediatrics, Torsion

Noncompaction cardiomyopathy (NCC) is a form of cardiomyopathy characterized by an expanded layer of trabeculations and deep intertrabecular recesses, in the inner ventricular muscle wall of the left ventricle.¹ This disease unfortunately lacks specific diagnostic criteria, leading to many normal individuals being diagnosed with NCC.² Therefore finding disease-specific characteristics that can differentiate patients with benign hypertrabeculations from those with true symptomatic NCC is crucial. The potential role of torsion as a diagnostic or

prognostic parameter in this disease has been studied infrequently in children, although recent reports in adults with NCC describe replacement of the normal wringing motion of the heart by a roller pump-like motion.^{3,4}

The normal wringing or twisting motion of the left ventricle during ejection consists of clockwise rotation of the base and counterclockwise rotation of the apex (when viewed from the apex). The roller pump-like motion found in some patients with NCC is characterized by rotation of the apex and base in the same clockwise direction. Hence, the wringing motion of the left ventricle is lost, and the left ventricle behaves like a roller pump. This motion has been labeled rigid body rotation or reverse apical rotation (RAR).^{5,6} How this abnormal rotation pattern affects ventricular function and whether it alters prognosis is not known.

Therefore, in this pilot study, we sought to describe the rotational mechanics of the left ventricle in children with isolated NCC during systole and diastole. We sought to investigate the association of RAR with history of NCC complications and with ventricular dysfunction. We hypothesized that compared to children with NCC and normal rotation, children with NCC and RAR would be more symptomatic, have

From the Division of Cardiology, The Children's Hospital of Philadelphia (H.M.N., A.E.M., P.Y., R.J.C.C.-A., T.S., M.J.O., K.D.M., A.B.), Philadelphia, Pennsylvania; Division of Pediatric Cardiology (H.M.N., J.I.E.H.), and Department of Pathology (P.C.U.), University of California, San Francisco, San Francisco, California.

Conflicts of Interest: None.

Reprint requests: Anirban Banerjee, MD, FACC, Division of Cardiology, The Children's Hospital of Philadelphia, 8NW-53, 3401 Civic Center Boulevard, Philadelphia, PA 19104 (E-mail: banerjeea@email.chop.edu).

0894-7317/\$36.00

Copyright 2018 by the American Society of Echocardiography. All rights reserved.

<https://doi.org/10.1016/j.echo.2018.02.015>

Abbreviations

EF = Ejection fraction
LV = Left ventricular
MRI = Magnetic resonance imaging
NCC = Noncompaction cardiomyopathy
RAR = Reverse apical rotation

more NCC-related complications, and manifest evidence of impaired left ventricular (LV) ejection and filling, secondary to loss of LV twist and untwist.

METHODS**Subject Enrollment**

We prospectively enrolled children being evaluated in the echocardiography laboratory at the Children's Hospital of

Philadelphia during diagnosis or routine follow-up of NCC if they were <18 years of age and had no associated congenital heart defects. Because of the low reproducibility⁷ and specificity² of the current echocardiographic diagnostic criteria for NCC, we only included patients who met all three echocardiographic criteria proposed by Jenni *et al.*,⁸ Stöllberger and Finsterer,⁹ and Chin *et al.*¹⁰ (For measurement techniques used, see Figure 1 and its legend.) Available cardiac magnetic resonance imaging (MRI) data were also evaluated for additional confirmation of the diagnosis of NCC.

A control group consisting of children with noncardiac chest pain, vasodepressor syncope, or functional heart murmur was also enrolled. Control subjects were approached for inclusion in the study if they had no evidence of structural heart disease, ejection fractions (EFs) > 55%, and no evidence of diastolic dysfunction on mitral inflow spectral Doppler or tissue velocities of the lateral mitral valve annulus. Subjects were excluded from the study if they had evidence of elevated pulmonary arterial pressure, on the basis of ventricular septal position or a tricuspid regurgitant jet >3 m/sec, elevated systemic blood pressure, or any arrhythmia at the time of the study.

Echocardiography

Complete transthoracic echocardiography was performed on all subjects to assess their eligibility for inclusion in the study on the basis of the criteria discussed earlier. To assess LV torsion, we used our published protocol for image acquisition.¹¹ Parasternal short-axis cine clips of the base of the heart at the level of the mitral valve leaflets and the apex of the heart were obtained. The cardiac apex was defined as the furthest apical extent of the LV cavity, distal to the base of the papillary muscles and just proximal to the level of cavity obliteration. A target frame rate of >60 Hz was achieved in all subjects. The timing of aortic valve closure and mitral valve opening was determined from

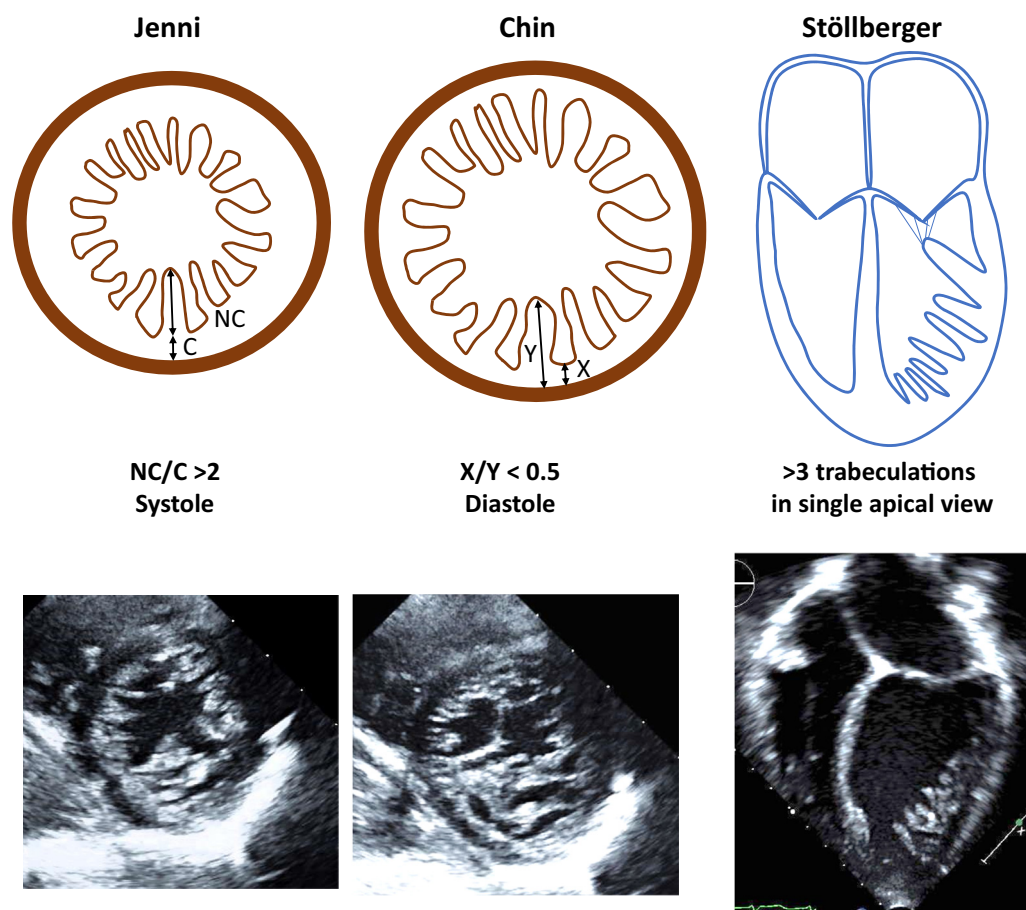


Figure 1 Schematic and two-dimensional echocardiographic images depicting the three methods used in the diagnosis of NCC (Jenni, Chin, and Stöllberger methods) from apical short-axis and four-chamber views. In the Jenni and Chin methods, the noncompacted segments are measured differently. In the Jenni method, the noncompacted segment is measured up to the bottom of the recesses (NC), whereas in the Chin method, it is measured up to the epicardium (Y). C and X are compacted segments for respective methods. The criteria for the diagnosis of NCC by the three methods are as follows: Jenni, NC/C ratio > 2; Chin, X/Y ratio < 0.5; and Stöllberger, more than three trabeculations in one imaging plane below the level the papillary muscles.

HIGHLIGHTS

- Rotational mechanics in children with noncompaction cardiomyopathy were studied.
- RAR in the clockwise direction occurred in 40% of children.
- Left ventricular dysfunction, heart failure, and arrhythmias were associated with RAR.
- Patients with premature untwisting during ejection had decreased ejection fraction.
- RAR is possibly related to dysfunction of the apical compacted layer of myocardium.

simultaneous mitral inflow and aortic outflow spectral Doppler interrogation. To compare the timing of rotation and torsion in relation to the events of the cardiac cycle in children with varying heart rates, we normalized the cardiac cycle length to systolic duration. This method allows systole (from the R wave on electrocardiography to aortic valve closure) to be designated as 0% to 100% and diastole (the rest of the cardiac cycle) as >100% (e.g., 110%, 120%). In this method, the timing of an event is divided by aortic valve closure time and multiplied by 100 to produce its timing in relation to end-systole (where end-systole = 100%). All studies were performed using a Philips iE33 ultrasound machine (Philips Medical Systems, Andover, MA).

Assessment of Distribution and Severity of Noncompaction

The segmental distribution and the severity of NCC in each segment using a 16-segment LV model were assessed qualitatively by an experienced investigator (A.B.). This was performed to evaluate if abnormal rotation was associated with a certain phenotype of NCC. The severity of NCC was graded on the basis of the depth of the recesses in each segment as follows: 0 = no trabeculations, 1 = shallow trabeculations, 2 = medium-sized trabeculations, and 3 = deep trabeculations. If a cardiac segment had two different severity scores when analyzed from two different views, the higher score was used for the analysis.

Speckle-Tracking Echocardiography

Speckle-tracking analysis was performed using the two-dimensional speckle-tracking software package 2D Cardiac Performance Analysis version 1.2.1.2 (TomTec Imaging Systems, Munich, Germany). The endocardial and epicardial borders of the left ventricle were traced. Of note, in the regions of noncompaction, the region of interest was placed at the base of the recesses, and the software tracked the base, not the tip, of the trabeculations. Tracking of the cardiac wall was examined visually on the cine images. The software generated rotation, rotation rate, and circumferential strain waveforms. Twist was calculated as peak value of isochronal apical rotation – basal rotation (deg) and torsion as twist/LV length (deg/cm). Untwist rate was defined as the peak rate of untwist (deg/sec). We also measured LV longitudinal strain in the four-chamber apical view of the heart. RAR was defined as rotation of the cardiac base and apex in the same clockwise direction during ejection. To account for differences in LV size among children of different ages, rotation and untwist rate were indexed to LV length at end-diastole.

Dyssynchrony

We evaluated systolic and diastolic dyssynchrony of the left ventricle to determine if dyssynchrony was associated with abnormal patterns of LV rotation. Systolic dyssynchrony was evaluated using the difference between the time to peak systolic velocity (s') of the medial and lateral mitral annuli using tissue Doppler. Diastolic dyssynchrony was evaluated using the difference between the time to peak early diastolic velocity (e') of the medial and lateral mitral annuli using tissue Doppler. Systolic dyssynchrony was defined as a time difference of >75 msec and diastolic dyssynchrony as a time difference of >15 msec on the basis of data published in the pediatric population by Friedberg *et al.*¹²

To assess interobserver variability, eight subjects with NCC and five control subjects were selected randomly, and the analysis was repeated de novo by a second investigator. To assess intraobserver variability, one observer (H.M.N.) repeated the measurements on the same subjects after 2 weeks.

This study was performed at the Children's Hospital of Philadelphia and approved by its institutional review board.

Statistical Analysis

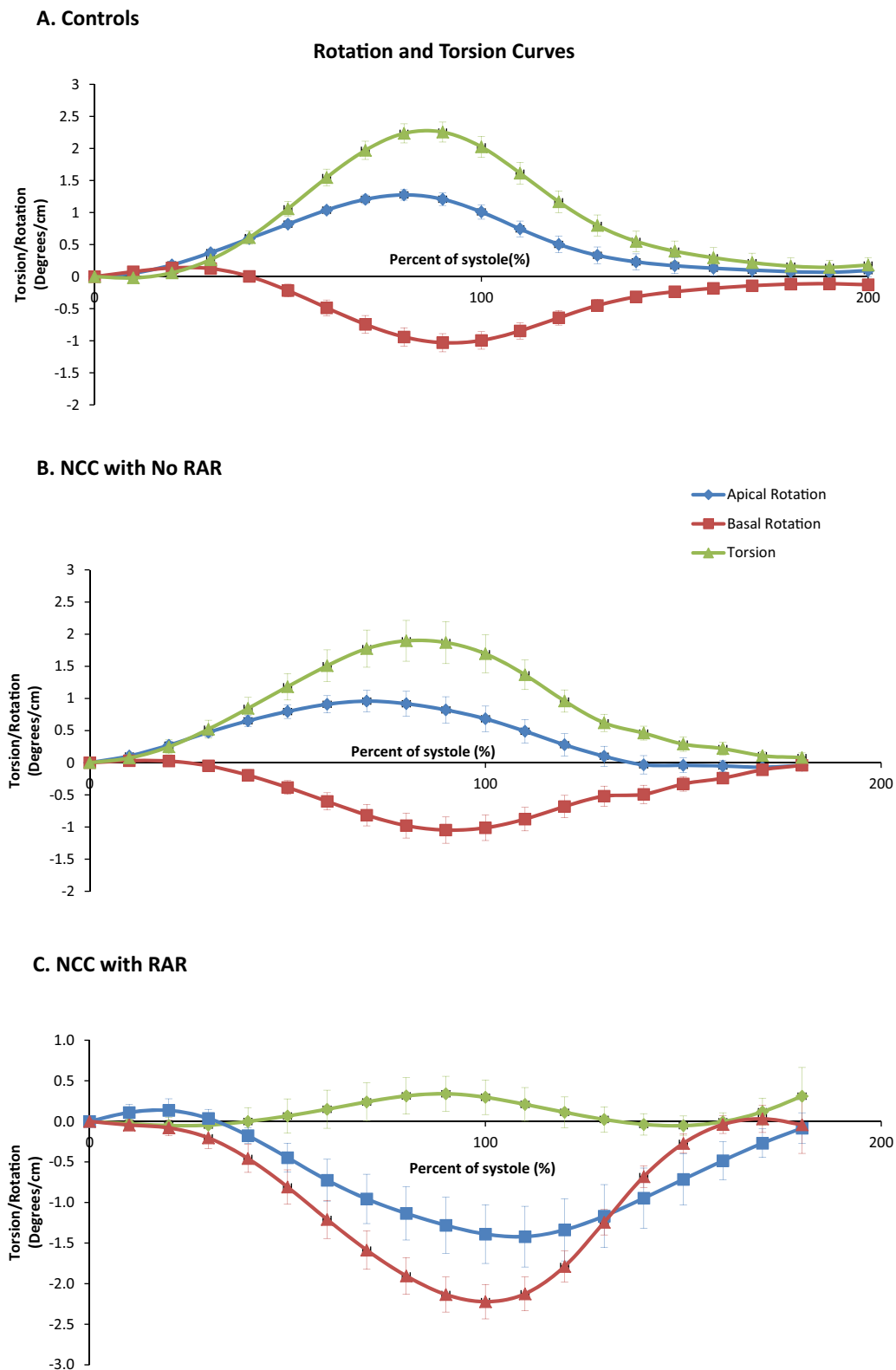
Data are expressed as median (interquartile range). Nonparametric testing was performed because of small sample size in each subgroup of patients with NCC. The Kruskal-Wallis test with the post hoc Dunn test and Bonferroni correction was used to assess differences among patients with NCC with RAR, patients with NCC without RAR, and control subjects. A χ^2 test and a Wilcoxon rank sum test were performed to compare the distribution and the severity of trabeculations in patients with RAR with those in patients without RAR, respectively. Intraclass correlation coefficients were used to assess intra- and interobserver variability. For all significance testing, a difference was considered significant at $P < .05$. The statistical analysis was performed using Stata version 13 (StataCorp, College Station, TX).

RESULTS**Study Population Demographics**

Thirty-one patients with NCC and 30 control subjects were recruited. Three patients and one control were excluded because of poor tracking. These four subjects had similar demographics as the rest of the subjects in the cohort. Hence, our cohort comprised 28 patients and 29 control subjects. The mean ages of the control subjects and the patients were 8.9 ± 5.4 and 7.6 ± 5.8 years, respectively ($P = .37$). Eleven patients had cardiac MRI studies that confirmed the diagnosis of NCC.

Rotation and Torsion Patterns in NCC

In our cohort of patients with NCC, we identified two patterns of rotation (Figures 2B and 2C). One was the normal rotation pattern, characterized by counterclockwise rotation of the apex and clockwise rotation of the base ($n = 17$ [61%]). Pattern 2 was RAR, in which the apex and base rotated in the same direction (i.e., clockwise; $n = 11$ [39%]). In one patient, the apex followed the base in an early counterclockwise rotation, followed by a clockwise rotation. This patient was included in the RAR group because the apex closely tracked the base and both rotated in the same direction.



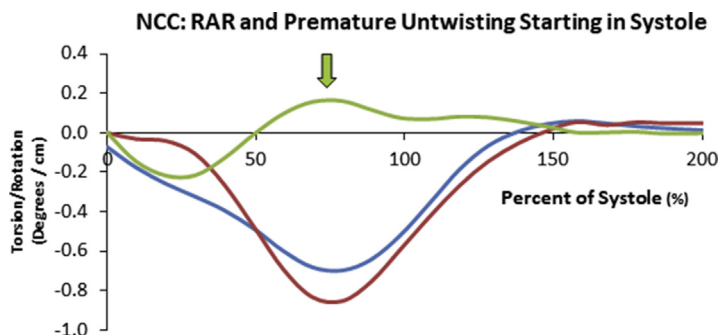


Figure 3 Curve plot depicting rotation and torsion in a patient with premature untwisting. End-systole coincides with the 100% mark. The *arrow* demonstrates the peak twist. Peak twist occurs very early in systole, and untwisting is complete by end-systole.

Table 1 Demographic characteristics and conventional echocardiographic measurements in patients with NCC and control subjects

Variable	Control subjects (n = 29)	NCC without RAR (n = 17)	NCC with RAR (n = 11)	P
Age (years)	8.2 (4.4–12.4)	7.4 (3.6–15.1)	3.1 (1.3–5.4)	.08
Female (%)	55	29.4	60	.53
BMI (kg/m ²)	17.4 (15.2–20.7)	20.4 (17.8–23.6)*	15.4 (14.2–19.5)	.04
Heart rate (beats/min)	87 ± 23.3	81.1 ± 22.4	90.5 ± 23.9	.67
SBP (mm Hg)	105.2 ± 14.4	105.1 ± 13	100.6 ± 12.2	.66
DBP (mm Hg)	60.7 ± 7.5	59.3 ± 8.8	62.2 ± 11.5	.72
LVEDD (cm)	3.8 (3.5–4.6)	4.1 (3.4–5.5)	3.8 (3.1–4.1)	.21
LVEDD Z score	-0.17 ± 0.96	0.75 ± 2.5	0.55 ± 1.1	.16
LVESD (cm)	2.4 (2.2–2.9)	2.7 (2.3–4.0)	2.7 (2.4–3.1)	.13
EF (%)	67 (65,70)	61 (58,67)*	53 (43,62)*	.001
EF < 50%	0 (0%)	1 (6%)	4 (36%)*†	<.001
E (m/sec)	0.91 (0.78–1.0)	1.0 (0.75–1.17)	0.9 (0.85–1.01)	.70
e' (m/sec)	0.13 (0.12–0.14)	0.1 (0.1–0.12)*	0.09 (0.07–0.1)*	.001
E/e'	6.8 (5.3–8.1)	8.6 (7–10.8)*	9.9 (4.9–13.1)*	.02

BMI, Body mass index; DBP, diastolic blood pressure; LVEDD, LV end-diastolic dimension; LVESD, LV end-systolic dimension; SBP, systolic blood pressure.

Data are expressed as mean ± SD and as median (interquartile range) for normal and non-normal distributions, respectively.

*P < .05 versus control subjects.

†P < .05 versus NCC without RAR.

Because torsion is an index derived from rotation, the different rotational patterns described above resulted in three different patterns of torsion: (1) Normal rotation with a normal torsion pattern ($n = 17$ [61%]; Figure 2B). (2) RAR with a normal torsion pattern. The torsion magnitude was low, but the timing to peak torsion was similar to that in control subjects ($n = 7$ [25%]; Figure 2C). (3) RAR with abrupt termination of torsion and premature untwisting, starting in early to mid-systole ($n = 4$ [14%]; Figure 3). Peak torsion occurred at 20% to 56% of systolic time ($P = .01$) during peak ejection. This was followed by premature untwisting with complete untwisting during the ejection phase of the cardiac cycle.

Rotation and Torsion Patterns and Clinical Characteristics

The demographic data of the control subjects and the NCC subgroups are shown in Table 1, and the clinical characteristics of the NCC subgroups are shown in Table 2. Four patients received medical care predominantly at another institution, so their medical

histories were incomplete. There was a trend toward younger patients in the RAR group ($P = .08$). Complications of NCC occurred in both patients with and those without RAR. However, patients with RAR were more likely to have histories of LV dysfunction (defined as an $EF < 50\%$ or symptoms of heart failure) and arrhythmias and were also more likely to be on heart failure medications, especially β -blockers. There were no patients with RAR who did not have histories of either LV dysfunction or arrhythmias. Five of the 11 patients with RAR presented with symptoms of heart failure, and three later developed symptoms of heart failure. The three remaining patients had histories of arrhythmias in the form of ventricular tachycardia, ventricular ectopy, or sinus bradycardia with ventricular ectopy.

Rotation and Torsion Patterns and Systolic Function

Patients with NCC had lower EFs than control subjects (Table 1). There was no statistically significant difference in EF between patients with NCC with or without RAR. However, patients with RAR were

Table 2 Clinical characteristics of patients with NCC with and without RAR

Patient characteristic	NCC without RAR (n = 13)	NCC with RAR (n = 11)	P
Familial	3 (24)	5 (55)	.24
Age at diagnosis			.49
Neonate (0–30 days)	3 (24)	2 (18)	
Infancy (31 days to 1 year)	3 (24)	6 (55)	
Childhood (>1 year)	7 (56)	3 (27)	
Not documented	4 (32)	0	
Presentation at diagnosis			
Murmur	3 (24)	0	.09
Arrhythmia/abnormal findings on electrocardiography	3 (24)	3 (27)	.81
Heart failure	2 (16)	5 (45)	.10
Syncope	1 (8)	1 (9)	.90
Screening	5 (40)	4 (36)	.92
Current NYHA class/Ross			.27
I	13 (100)	10 (91)	
II	0	1 (9)	
III	0	0	
IV	0	0	
Complications			
History of LV dysfunction	3 (24)	8 (73)	.02
Arrhythmias	1 (8)	6 (55)	.04
Thromboembolic	1 (8)	0	.55
Medications			
Diuretic	0	1 (9)	.27
ACE inhibitor	3 (24)	7 (64)	.24
β -blocker	2 (16)	6 (55)	.02
Digoxin	2 (16)	0	.17
Spironolactone	2 (16)	2 (18)	.44
Any of the above medications	4 (32)	10 (91)	.003

ACE, Angiotensin-converting enzyme; NYHA, New York Heart Association.

Data are expressed as number (percentage).

more likely to have EFs < 50% than patients without RAR (Table 1). Because torsion, rather than rotation, is the motion responsible for ejection, we studied the association between presence of an abnormal torsion pattern (pattern 3 depicted in Figure 3) and EF. Patients with abnormal torsion pattern (RAR and premature untwisting) had lower EFs (46% [interquartile range, 43%–52%]) than all other patients with NCC [61% (57%, 67%)], $P = .006$.

Rotation and Torsion Patterns and Diastolic Function

Patients with NCC had lower lateral mitral annular velocities and higher E/e' ratios than control subjects (Table 1). Patients with NCC with RAR had slower untwist rates than control subjects (Table 3 and Figure 4, red vs orange arrows). In contrast, patients with NCC without RAR had similar untwist rates as control subjects

(Table 3 and Figure 4, green vs blue arrows). Patients with premature untwisting pattern finished most of the untwisting during systole (range, 64%–89% of systole; Figure 4, red arrow)

Rotation and Torsion Patterns and LV Strain

The average longitudinal strain measured in the four-chamber view in the RAR group was lower than that in both patients without RAR and in the control group (Table 3). Circumferential strain was not uniform among the different segments of a normal left ventricle. Control patients manifested a known circumferential strain gradient, characterized by higher strain at the LV apex than at the base. In patients with NCC, circumferential strain at the cardiac apex and base was lower than in control subjects (Table 3). There was a more prominent decrease in circumferential strain at the apex compared with that at the base in patients with NCC. Therefore, in patients with NCC, the apex-to-base circumferential strain gradient was either significantly decreased or reversed. This decrease or reversal of the LV circumferential strain gradient was more pronounced in the patients with NCC with RAR (Table 3).

Rotation Pattern and NCC Phenotype

The apical segments were the most commonly and most severely affected by noncompaction. The basal segments and the midseptal and midanteroseptal segments were less commonly and less severely affected. There were no differences in the distribution or the severity of noncompaction between the patients with RAR and those without RAR (Figure 5).

Rotation and Torsion Pattern and Dyssynchrony

Systolic dyssynchrony occurred in only one patient with RAR (9%), and diastolic dyssynchrony occurred in two patients (14%) with no RAR and in six patients (55%) with RAR. Therefore, patients with RAR exhibited more diastolic dyssynchrony ($P = .03$). Three of the four patients with premature untwisting exhibited diastolic dyssynchrony.

Intraobserver and Interobserver Variability

The intraobserver and interobserver agreement for the patterns of rotation was 100%. In control subjects, the intraclass correlation coefficients for intraobserver and interobserver variability for apical rotation were 0.94 and 0.97, respectively, and for basal rotation were 0.81 and 0.84, respectively. In patients with NCC, the intraclass correlation coefficients for intraobserver and interobserver variability for apical rotation were 0.88 and 0.71, respectively, and for basal rotation were 0.92 and 0.97, respectively.

DISCUSSION

To our knowledge this is the first study to investigate LV rotational patterns in children with NCC. We found that 39% of children diagnosed with NCC had RAR patterns during ejection. LV torsion and untwist rate were decreased in this subgroup of patients with RAR. This group of patients had histories consistent with a more severe phenotype of NCC, yet by no means were complications of NCC exclusive to this group of patients. Four patients with RAR had early termination of LV twist before mid-systole with premature untwisting and almost full completion of untwisting by the end of systole. This latter group of patients with NCC, RAR, and premature untwisting had lower EFs than both control subjects and other patients with NCC.

Table 3 LV speckle-tracking-derived strain measurements in patients with NCC and control subjects

Variable	Control subjects (n = 29)	NCC without RAR (n = 17)	NCC with RAR (n = 11)	P
Rotational strain				
Apical rotation (°)	7.9 (6.2 to 10.2)	7.1 (3.8 to 9.2)	-4.1* (-3.6 to -6.3)	.009
Apical rotation indexed to LV length (°/cm)	1.4 (1.1 to 1.6)	0.9 (0.7 to 1.6)	-0.7* (-0.5 to -1.3)	.04
Basal rotation (°)	-7.3 (-6.1 to -8.9)	-7.5 (-5.6 to -9.2)	-6.2 (-4.9 to -9.0)	.73
Basal rotation indexed to LV length (°/cm)	-1.2 (-1.0 to -1.6)	-1.2 (-0.7 to -1.6)	-1.2 (-1.1 to -1.6)	.76
Twist (°)	15.5 (12.3 to 17.5)	13.1 (11.1 to 17.1)	3.9 [†] (1.8 to 6.6)	<.001
Torsion (°/cm)	2.5 (2.0 to 2.9)	2.1 (1.5 to 3.4)	0.7 [†] (0.3 to 1.3)	<.001
Untwist rate (°/sec)	105 (92.3 to 138)	86.8 (68.1 to 144.1)	33.4 [†] (19 to 76.1)	<.001
Untwist rate indexed to LV length (°/sec/cm)	17.9 (15 to 21.5)	14.1 (9.2 to 24)	8.4 [†] (3.6 to 15.6)	.002
Circumferential strain				
Circumferential strain, apex	-29.9 (-26.9 to -32.5)	-21.8* (-19.0 to -24.5)	-18.1* (-17.1 to -21.3)	<.001
Circumferential strain, base	-23.4 (-20.2 to -25.7)	-19.9* (-15.5 to -21.8)	-18.0* (-14.9 to -20.5)	.004
Circumferential strain, apex-base gradient	-6.7 (-10.7 to -3.1)	0.2* (-3.6 to 4.6)	2.3* (-1.8 to 3.3)	.002
Longitudinal strain				
LV longitudinal strain (%)	-19.9 (-18.7 to -21.2)	-19 (-14.5 to -21.9)	-15.6* (-12.9 to -19.3)	.01

Data are expressed as median (interquartile range). Torsion and twist are presented as absolute values, while negative rotation is clockwise and positive rotation is counterclockwise.

**P* < .05 versus control subjects.

[†]*P* < .05 versus NCC without RAR.

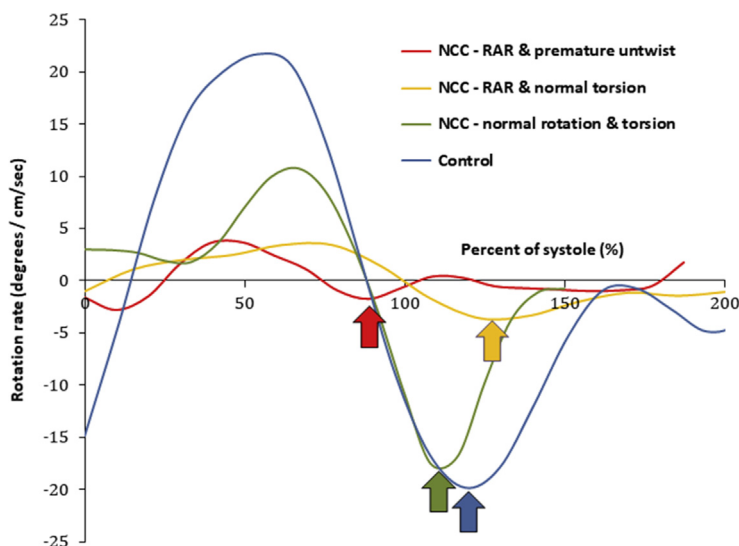


Figure 4 Curve plot depicting rotation and untwist rate in control subjects and patients with NCC. End-systole coincides with the 100% mark. The arrows demonstrate the peak untwist rate. The magnitude of peak untwist rate is related to the rotation pattern, while the timing of the untwist rate is related to the torsion pattern.

Mechanisms of RAR

In the normal left ventricle, the subepicardial fibers form left-handed helices, which rotate the apex counterclockwise. The subendocardial fibers form right-handed helices that rotate the apex clockwise. The subepicardial fibers are longer and generate greater torque than the

shorter subendocardial fibers. Therefore, the subepicardial fibers dominate the rotation of the apex, resulting in a net counterclockwise rotation of the apex¹³ (Figure 6A). Any process that disrupts the balance between the torques of the subepicardial and the subendocardial fibers can theoretically affect rotation and consequently torsion.

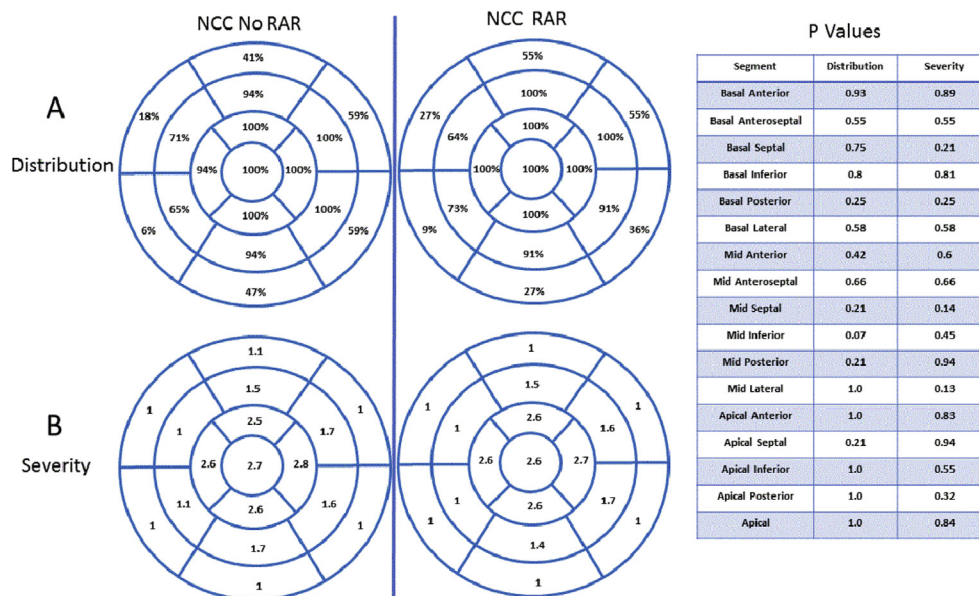


Figure 5 Bull's-eye diagram depicting the distribution and severity of trabeculations in patients with NCC, with and without RAR. The distribution diagram (**A**) depicts the percentage of patients with noncompaction of each cardiac segment. The severity diagram (**B**) depicts the average severity score of each cardiac segment. There were no significant differences between the two groups with regard to both the distribution and the severity of hypertrabeculations, as shown in the table of *P* values.

Apical Dysfunction. In this study, we tried to investigate the processes that may explain the occurrence of RAR. We found apical circumferential strain in patients with NCC to be significantly decreased. This finding was more profound in patients with RAR. The decrease in apical circumferential strain resulted in the decrease, loss, or even reversal of the normal increase in circumferential strain from the base to the apex (Table 3). Because rotation is a shear strain between longitudinal and circumferential normal strain,¹⁴ such a significant change in circumferential strain between the apex and the base (along with a decrease in global longitudinal strain present in patients with RAR) can potentially lead to major changes in rotation.

Role of Compacted Layer. It is unclear why apical clockwise rotation occurs in NCC. The logical thinking would be that in NCC, the inner (trabeculated) part of the LV wall is not contracting, hence it is likely that this segment is not contributing to myocardial deformation. However, if that were the case, one would expect to find normal or exaggerated apical counterclockwise rotation due to the loss of subendocardial fiber function that normally counteracts the subepicardial fiber function. Failure to observe this exaggerated apical counterclockwise rotation suggests that the subepicardial layer rather than the subendocardial layer may be a culprit. We speculate that apical rotational dysfunction occurs in NCC, not only because of the impaired subendocardial component of the myocardial contraction but secondary to additional dysfunction of the compacted outer layer. A cardiac MRI study in children with NCC demonstrated the presence of late gadolinium enhancement in compacted segments, further supporting our conjecture that pathologic changes may extend beyond the noncompacted layer.¹⁵

We were unable to find a correlation between the severity or the distribution of the trabeculations and the pattern of contraction,

also suggesting a lesser role played by the noncompacted zone. However, there are contradictory reports on the effect of the distribution and severity of trabeculations in NCC on myocardial mechanics.¹⁶⁻¹⁹

Abnormal Myofiber Orientation. One possible structural explanation for this apical dysfunction is shown in Figure 6B, which illustrates that the compacted myocardium shows disarray of the myofiber orientation. Figure 6B is a photomicrograph taken from a 21-week gestation fetal left ventricle with NCC, cut in a plane parallel to the short axis, and a similar section from the normal heart of an age-matched control. In normal cardiac development, this stage is long after the LV myocardium has become compact, having only a narrow trabecular layer at the endocardial surface.²⁰ Normally the outer layers of LV myocardium are almost longitudinal and manifest an orderly array (Figure 6B, images A and B). In contrast, subepicardial myofibers in NCC manifest a more disorderly orthogonal array, with increased interstitial collagen (Figure 6B, images C and D). In these short-axis views, some of the myofibers are seen in cross-section, while other myofibers are circumferential. A schematic representation of the myofibers is depicted in Figure 6A. It is noteworthy that by presenting this photomicrograph (Figure 6B), we are not claiming scientific proof of the mechanism of RAR but merely pointing out an interesting finding in a rare disease, for which histologic data are even rarer in the scientific literature. A single case report in an adult with NCC also showed myocardial fiber disarray and increased extracellular matrix.²¹

We also tested another hypothesis that may theoretically cause RAR. Myocardial activation starts from the endocardium to the epicardium, and thus disruption of the inner layers of the myocardium can understandably affect the sequence of myocardial

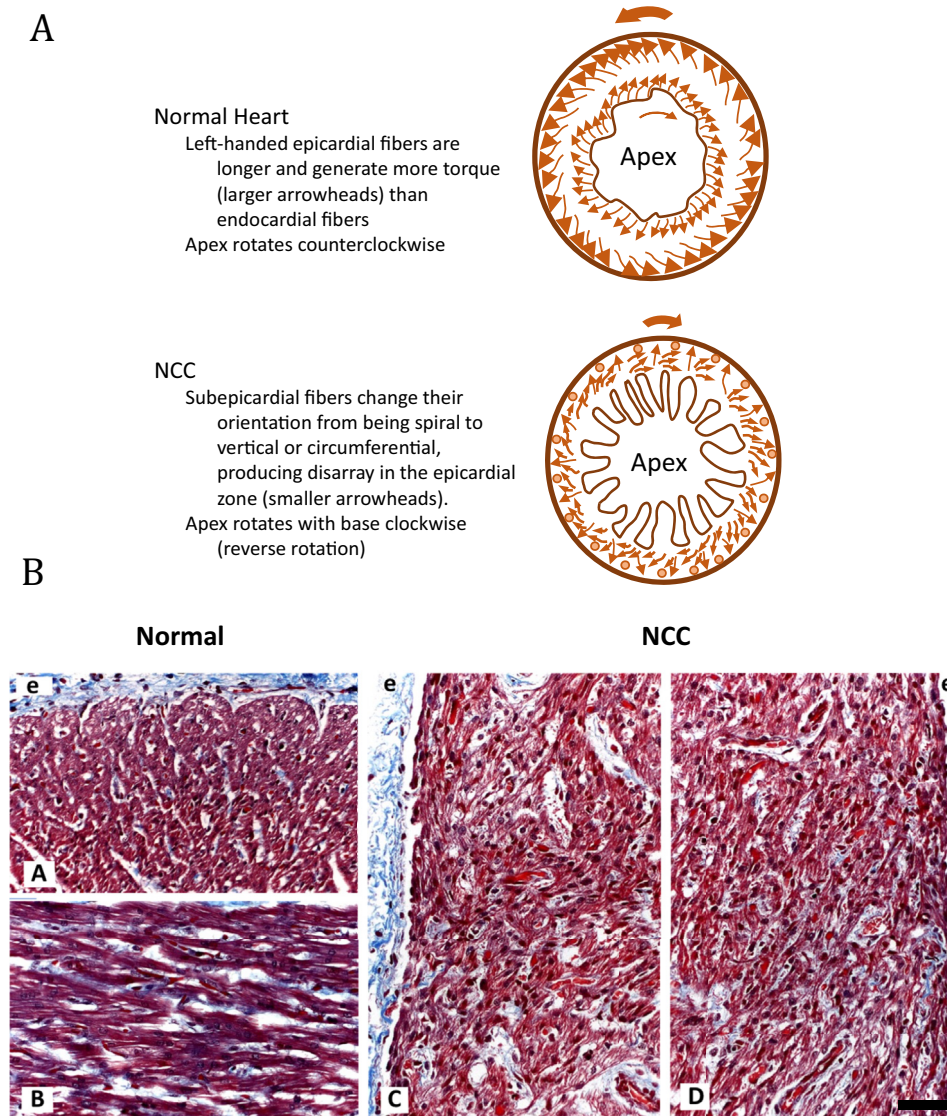


Figure 6 (A) Schematic diagram of the LV apex viewed from the apex to the base in normal and NCC hearts. In the normal heart, the left-handed subepicardial fibers are longer and generate more torque (larger *arrowheads*) than the subendocardial fibers. This results in the apex rotating counterclockwise. In NCC, subepicardial fibers change their orientation from spiral to vertical or circumferential, producing disarray in the subepicardial zone. This may explain the apex rotating clockwise (reverse rotation) in NCC. (B) Comparison of myofiber orientation in a 21-week gestation fetal left ventricle with NCC versus a normal heart. In a short-axis slice of the normal fetal heart (*images A and B*), high magnification discloses subepicardial myofibers (red cross-sectioned myofibers in *image A*) coursing in parallel along the long axis, with scant collagen (*blue*); midmyocardial fibers are circumferential (longitudinally sectioned in *image B*). In contrast, a fetal heart with LV noncompaction (*images C and D*) has subepicardial myofibers (red) in orthogonal array (*image C*), with increased interstitial collagen (*blue*). The relative disarray is also reflected in the midmyocardial fibers (*image D*). *e*, Epicardium. Gomori trichrome stain, calibration bar = 50 μm .

activation. We found no evidence of systolic dyssynchrony, which could have explained the abnormal rotational patterns. On the other hand, we found significant diastolic dyssynchrony, which is possibly the effect rather than the cause of RAR.

Systolic Function

Regardless of the cause behind the abnormal rotation, patients with solely RAR and normal torsional pattern (pattern 2 under "Results"; [Figure 2C](#)) did not have lower EFs than control subjects. Therefore, even though the magnitude of torsion was dramatically decreased

in this pattern, the left ventricle was still able to maintain its EF. These findings raise the question regarding what other mechanisms are at play that compensate for impaired torsion. A lower EF was seen only in the group of patients in whom torsion was terminated early during ejection.

Diastolic Function

In our cohort, patients with RAR exhibited two mechanisms for abnormal LV untwisting that could affect ventricular filling. One was a marked decrease in untwist rate. The other was complete

untwisting before the start of isovolumic relaxation (pattern 3, depicted in Figure 3), thereby losing the contribution of untwisting to ventricular filling. Further investigations are needed to assess the contribution of abnormal rotation and torsion to ventricular diastolic dysfunction.

Clinical Implications of Hypertrabeculations

Technological advances in image resolution have led to a more intricate visualization of the LV myocardium, resulting in overdiagnosis of NCC. This has resulted in the use of cardiac MRI as the “gold standard” for NCC diagnosis.²² However, a 10-year follow-up study of 706 asymptomatic individuals with LV hypertrabeculations demonstrated that they did not have progressive deterioration in LV function during this period, even if they met MRI diagnostic criteria for NCC.²³ Therefore, new diagnostic and prognostic criteria for NCC are clearly needed. Our study suggests that a criterion derived from LV deformation used in conjunction with morphologic criteria may help confirm NCC in patients with LV hypertrabeculations.

Limitations

The main limitation of our study was the small sample size. This precluded any further subgroup analyses of different torsional patterns. However, NCC is a rare disease in children. In the registry of the National Australian Childhood Cardiomyopathy Study, there were 314 new cases of cardiomyopathy in a 10-year period, with only 29 patients with NCC from Australia.²⁴ Our study was a pilot study from a single center. The number of patients studied in our single-center study was comparable with the number of patients in the Australian registry. However, larger multicenter studies are needed to validate these preliminary findings and generate diagnostic and prognostic data.

Another limitation of our study is that we did not extensively analyze dyssynchrony using all of the cardiac segments but used the difference between the time to peak systolic velocity (s') of the medial and lateral mitral annuli. This method may have underestimated the degree of dyssynchrony in our cohort.

CONCLUSIONS

Almost half of the children with NCC exhibit RAR. Complications of NCC are more common in this subgroup of patients. Therefore, RAR may be of prognostic value in NCC, rather than a diagnostic sign for NCC. Premature untwisting of the left ventricle is a more worrisome sign, which is associated with decreased EF in patients with NCC.

REFERENCES

1. Maron BJ, Towbin JA, Thiene G, Antzelevitch C, Corrado D, Arnett D, et al. Contemporary definitions and classification of the cardiomyopathies: an American Heart Association Scientific Statement from the Council on Clinical Cardiology, Heart Failure and Transplantation Committee; Quality of Care and Outcomes Research and Functional Genomics and Translational Biology Interdisciplinary Working

- Groups; and Council on Epidemiology and Prevention. *Circulation* 2006;113:1807-16.
2. Kohli SK, Pantazis AA, Shah JS, Adeyemi B, Jackson G, McKenna WJ, et al. Diagnosis of left-ventricular non-compaction in patients with left-ventricular systolic dysfunction: time for a reappraisal of diagnostic criteria? *Eur Heart J* 2008;29:89-95.
3. Van Dalen BM, Caliskan K, Soliman OI, Kauer F, van der Zwaan HB, Vletter WB, et al. Diagnostic value of rigid body rotation in noncompaction cardiomyopathy. *J Am Soc Echocardiogr* 2011;24:548-55.
4. Peters F, Khandheria BK, Libhaber E, Maharaj N, Santos dos C, Matioda H, et al. Left ventricular twist in left ventricular noncompaction. *Eur Heart J Cardiovasc Imaging* 2013;15:48-55.
5. Nemes A, Kalapos A, Domsik P, Forster T. Identification of left ventricular “rigid body rotation” by three-dimensional speckle-tracking echocardiography in a patient with noncompaction of the left ventricle: a case from the MAGYAR-Path study. *Echocardiography* 2012;29:E237-40.
6. Popescu BA, Beladan CC, Călin A, Muraru D, Deleanu D, Roșca M, et al. Left ventricular remodelling and torsional dynamics in dilated cardiomyopathy: reversed apical rotation as a marker of disease severity. *Eur J Heart Fail* 2009;11:945-51.
7. Saleeb SF, Margossian R, Spencer CT, Alexander ME, Smoot LB, Dorfman AL, et al. Reproducibility of echocardiographic diagnosis of left ventricular noncompaction. *J Am Soc Echocardiogr* 2012;25:194-202.
8. Jenni R, Oechslin E, Schneider J, Attenhofer Jost C, Kaufmann PA. Echocardiographic and pathoanatomical characteristics of isolated left ventricular non-compaction: a step towards classification as a distinct cardiomyopathy. *Heart* 2001;86:666-71.
9. Stöllberger C, Finsterer J. Left ventricular hypertrabeculation/noncompaction. *J Am Soc Echocardiogr* 2004;17:91-100.
10. Chin TK, Perloff JK, Williams RG, Jue K, Mohrmann R. Isolated noncompaction of left ventricular myocardium. A study of eight cases. *Circulation* 1990;82:507-13.
11. Nawaytou HM, Yubbu P, Montero AE, Nandi D, O'Connor MJ, Shaddy RE, et al. Left ventricular rotational mechanics in children after heart transplantation. *Circ Cardiovasc Imaging* 2016;9:e004848.
12. Friedberg MK, Roche SL, Mohammed AF, Balasingam M, Atenafu EG, Kantor PF. Left ventricular diastolic mechanical dyssynchrony and associated clinical outcomes in children with dilated cardiomyopathy. *Circ Cardiovasc Imaging* 2008;1:50-7.
13. Buckberg GD, Hoffman JIE, Coghlan HC, Nanda NC. Ventricular structure-function relations in health and disease: part I. The normal heart. *Eur J Cardiothorac Surg* 2015;47:587-601.
14. Modesto K, Sengupta PP. Myocardial mechanics in cardiomyopathies. *Prog Cardiovasc Dis* 2014;57:111-24.
15. Cheng H, Lu M, Hou C, Chen X, Li L, Wang J, et al. Comparison of cardiovascular magnetic resonance characteristics and clinical consequences in children and adolescents with isolated left ventricular non-compaction with and without late gadolinium enhancement. *J Cardiovasc Magn Reson* 2015;17:44.
16. Kalapos A, Domsik P, Forster T, Nemes A. Left ventricular strain reduction is not confined to the noncompacted segments in noncompaction cardiomyopathy—insights from the three-dimensional speckle tracking echocardiographic MAGYAR-Path study. *Echocardiography* 2014;31:638-43.
17. Caliskan K, Soliman OI, Nemes A, van Domburg RT, Simoons ML, Geleijnse ML. No relationship between left ventricular radial wall motion and longitudinal velocity and the extent and severity of noncompaction cardiomyopathy. *Cardiovasc Ultrasound* 2012;10:9.
18. Tufekcioglu O, Aras D, Yildiz A, Topaloglu S, Maden O. Myocardial contraction properties along the long and short axes of the left ventricle in isolated left ventricular non-compaction: pulsed tissue Doppler echocardiography. *Eur J Echocardiogr* 2008;9:344-50.
19. Dellegrottaglie S, Pedrotti P, Roghi A, Pedretti S, Chiariello M, Perrone-Filardi P. Regional and global ventricular systolic function in isolated

- ventricular non-compaction: pathophysiological insights from magnetic resonance imaging. *Int J Cardiol* 2012;158:394-9.
20. Bartram U, Bauer J, Schranz D. Primary noncompaction of the ventricular myocardium from the morphogenetic standpoint. *Pediatr Cardiol* 2007; 28:325-32.
 21. Pujadas S, R Bordes R, Bayes-Genis A. Ventricular non-compaction cardiomyopathy: CMR and pathology findings. *Heart* 2005;91:582.
 22. Petersen SE, Selvanayagam JB, Wiesmann F, Robson MD, Francis JM, Anderson RH, et al. Left ventricular non-compaction: insights from cardiovascular magnetic resonance imaging. *J Am Coll Cardiol* 2005;46:101-5.
 23. Zemrak F, Ahlman MA, Captur G, Mohiddin SA, Kawel-Boehm N, Prince MR, et al. The relationship of left ventricular trabeculation to ventricular function and structure over a 9.5-year follow-up: the MESA study. *J Am Coll Cardiol* 2014;64:1971-80.
 24. Nugent AW, Daubeney PEF, Chondros P, Carlin JB, Cheung M, Wilkinson LC, et al. The epidemiology of childhood cardiomyopathy in Australia. *N Engl J Med* 2003;348:1639-46.